Free Radical Research, January 2006; 40(1): 41–52

Taylor & Francis
Taylor & Francis Group

Exogenous *N*-linoleoyl tyrosine marker as a tool for the characterization of cellular oxidative stress in macrophages

ANDREA SZUCHMAN[1,2], MICHAEL AVIRAM[2], KHATIB SOLIMAN[1], SNAIT TAMIR[1], & JACOB VAYA[1]

[1]*Laboratory of Natural Medicinal Compounds, Migal-Galilee Technological Center, Kiryat Shmona and Tel-Hai Academic College, Kiryat Shmona, Israel, and* [2]*The Lipid Research Laboratory, Technion Faculty of Medicine, The Rappaport Family Institute for Research in the Medical Sciences and Rambam Medical Center, Haifa, Israel*

Accepted by Professor M.J. Davies

(Received 16 May 2005; in revised form 12 July 2005)

Abstract

Oxidative stress and its resultant products continue to attract investigators. Numerous endogenous substances have been suggested as potential markers for the identification of oxidative stress in tissues and organisms. In this study, we present a novel concept whereby an exogenous marker is designed and synthesized for the characterization of oxidative stress. The designed marker is constructed from tyrosine (Tyr) and linoleic acid (LA), which are attached covalently to form *N*-linoleoyl tyrosine (*N*-LT). Each of the two components (Tyr and LA) is known to be easily oxidized upon exposure to different types of reactive species. Combining the two allows their distinction from the endogenous Tyr and LA in the tested biological samples. The ability of the *N*-LT marker to characterize oxidative stress in macrophage cell lines was first studied using different types of ROS/RNS. *N*-LT was found to interact with macrophages, binding to the cell membrane. Upon treatment of J-774 A.1 macrophages with *N*-LT (40 μM) and with various oxidants; HOCl (0.2, 0.4 mM), copper ions (20 μM), SIN-1 (0.1, 1.0 mM), specific oxidized *N*-LT (Ox-*N*-LT) products were formed, depending on the type of oxidant used. Exposing cells to HOCl (0.2 mM) resulted in exclusive attack of the LA residue of *N*-LT, preferentially forming an adduct of HOCl to the LA double bond (*N*-L(HOCl)T, 4.3%). In contrast, when SIN-1 (0.1 mM) was applied as the oxidant, the Tyr moiety of *N*-LT was most reactive, yielding a nitration product of the Tyr aromatic ring (*N*-LT(NO_2), 1.8%). Similar *N*-LT oxidation in cell-free systems yielded a significantly higher content of Ox-*N*-LT (10.8% *N*-L(HOCl)T, 7% *N*-LT(NO_2)). The designed marker was then tested with peritoneal macrophages taken from atherosclerotic apolipoprotein-deficient (E^0) mice showing specific and selective oxidation of *N*-LT to yield *N*-LT-hydroperoxide (1.9% *N*-L(OOH)T), at significantly higher levels than resulted from similar experiments using peritoneal macrophages harvested from control BalbC mice (0.0% *N*-L(OOH)T). In contrast, the differences in *N*-L(epoxy)T level between BalbC and E^0 mice were not significant using both types of peritoneal macrophages (E^0 and BalbC), suggesting that *N*-L(OOH)T is characteristic of the atherosclerotic state. Thus, we show that the designed marker is sufficiently sensitive to detect oxidative stress imposed on cells and cell-free systems and to react selectively with the various ROS/RNS induced. Such a marker may be useful for characterizing oxidative stress in general, and possibly also in oxidative-stress-associated diseases.

Keywords: *Oxidative stress, marker, tyrosine, linoleic acid, free radical, hypochlorous acid*

Introduction

Oxidative stress is known to be involved in several human diseases, such as cardiovascular disease, cancer, inflammation-related diseases and aging [1–3]. Reactive oxygen and nitrogen species (ROS/RNS), such as superoxide ($O_2^{\cdot-}$), hydrogen peroxide (H_2O_2), hydroxyl radical ($HO^{\cdot}$), nitrogen oxide ($NO^{\cdot}$), peroxynitrite ($ONOO^-$) and hypochlorous acid (HOCl), are all products of normal metabolic

Correspondence: J. Vaya, Laboratory of Natural Medicinal Compounds, Migal-Galilee Technology Center, P.O. Box 831, Kiryat Shmona 11016, Israel. Tel: 972 4 6953512. Fax: 972 4 6944980. E-mail: vaya@migal.org.il

ISSN 1071-5762 print/ISSN 1029-2470 online © 2006 Taylor & Francis
DOI: 10.1080/10715760500358787

pathways in humans which may either be useful (e.g. in the destruction of invading organisms) or cause unwanted collateral damage to normal neighboring cells [4]. ROS/RNS also take part in signaling cascades and are involved in cellular functions such as cell proliferation, inflammation and adhesion. Under certain conditions, ROS/RNS exert harmful effects [5]. Thus, the identification of reliable biomarkers in cells, tissues and organisms under oxidative stress has become essential for predicting the early development of pathological conditions. Many methods are available to measure reactive species (RS) and oxidative damage. Some of them attempt to trap these species (ESR, for example [6,7]), while others try to measure the levels of the oxidative damage, such as by measuring peroxide values (PD), or the levels of thiobarbituric reactive substances (TBARs), isoprostanes, protein carbonyls and oxo-guanosine [3,8]. However, such biomarkers and the proposed methods bear some limitations: Some are not specific, measuring uncharacterized products of oxidative stress, whereas others' application *in vivo* is questionable [2].

The objective of the present study was to suggest and test a newly designed marker for oxidative stress that would enable the measurement of stress levels, an identification of the type of ROS/RNS involved, and a characterization of the damaged products. The designed marker consists of the amino acid tyrosine (Tyr) and the polyunsaturated fatty acid (PUFA) linoleic acid (LA), forming *N*-linoleoyl tyrosine (*N*-LT). This molecule contains both a lipophilic subunit (the LA), which can enter into the lipophilic tissues and membranes, and hydrophilic subunits, the carboxylic group as well as the hydroxyl phenol. The LA and Tyr molecules are known to be easily oxidized under oxidative stress and to generate specific oxidized products, depending on the type of ROS/RNS present *in vivo*. For example, Tyr can be attacked by reactive chloride, bromide and nitrogen species, giving products such as 3-chlorotyrosine, 3,5-dichlorotyrosine, 3-bromotyrosine and 3-nitrotyrosine. These oxidative products have been detected in the plasma, low-density lipids (LDL) and atherosclerotic plaques [9–13]. Peroxidation of LA gives different hydroperoxides [14,15], and the reaction of nitrogen- and chloride-RS yields different lipid chlorohydrins and nitration products [16–18]. The use of *N*-LT constructed from Tyr and LA enabled us to distinguish them and their oxidized products from the endogenous Tyr and LA of the tested sample, and to determine when they are formed. Thus, an analysis of the oxidative-stress-dependent fingerprint of the oxidized tyrosine-linoleate (Ox-*N*-LT) products may enable an in-depth investigation of the oxidative stress process in cells and tissues and may clarify the association between pathological conditions and oxidative fingerprints.

Materials and methods

Materials

LA, *N-t*-BOC-L-tyrosine (tyrosine-BOC), 3-chlorotyrosine, 3-nitrotyrosine, *N,O*-bis(trimethylsilyl) acetamide (BSA), ethylenediaminetetraacetic acid (EDTA), butylated hydroxytoluene (BHT), sodium hypochlorite (NaOCl), triphenylphosphine, *N*-bromosuccinimide (NBS), pyridine and XTT (sodium 3′-[1-[(phenylamino)-carbonyl]-3,4-tetrazolium]-bis(4-methoxy-6-nitro)benzene-sulfonic acid hydrate) were purchased from Sigma Chemical Co. (St Louis, MO). 3-Morpholinosydnonimine (SIN-1) was obtained from acros organics. Phosphate buffer saline (PBS), Dulbecco's modified Eagle's medium (DMEM), RPMI-1640 medium, Hank's balanced salt solution (HBSS), fetal calf serum (FCS; heat-inactivated at 56°C for 30 min) penicillin, streptomycin, nystatin, L-glutamine and sodium pyruvate were obtained from Biological Industries (Beit Haemek, Israel).

The synthesis of N-*LT (Figure 1)*

Tyrosine methyl ester (2). Two milliliter of concentrated (96%) H_2SO_4 were added drop-wise to a heterogenic solution of Tyr (1) (2 g, 11 mmol) in methanol (30 ml). The mixture was refluxed for 4 h, and the solution was concentrated by evaporating to half its volume, triturated with a saturated solution of sodium carbonate to a pH of ~10 and extracted with dichloromethane. The organic phase was evaporated to a white solid (1.5 g, 7.68 mmol) (70% yield), which was identified by FTIR, UV, LC/MS and NMR as Tyr methyl ester.

N-*linoleoyl tyrosine methyl ester (3) [19]*. NBS (1.25 g, 7 mmol) was added in one portion to a stirred solution of triphenylphosphine (1.71 g, 6.5 mmol) and LA (1.71 g, 6.10 mmol) in dried dichloromethane (5 ml) at 0°C and the temperature was allowed to reach 25°C. This solution was added drop-wise to a second solution of Tyr methyl ester (2) (1.14 g, 5.9 mmol) and pyridine in dried dichloromethane at 0°C. The mixture was allowed to reach room temperature, and the solvents were evaporated to give a crude material which was chromatographed on a silica gel, using hexane–acetone (70:30, v/v) as the eluent to give pure *N*-LT methyl ester (3) (2.5 g, 5.5 mmol) at a yield of 94% with a molecular mass of 456.7 (M^{-1}) by LC/MS. ^{1}H-NMR analysis ($CDCl_3$, 200 mHz) δ_{ppm} results; 6.89(d, 2H); 6.67(d, 2H); 5.87(d, 2H); 5.31(m, 4H); 4.8(q, 1H); 3.71(s, 3H); 3.00(m, 2H); 2.74(t, 3H); 2.14(t, 2H); 2.00(m, 4H); 1.59(m; 4H); 1.25(s, 14H), 0.82(d, 2H). IR (neat) ν_{max} 3352, 2925, 1736, 1655, 1517, 1448.

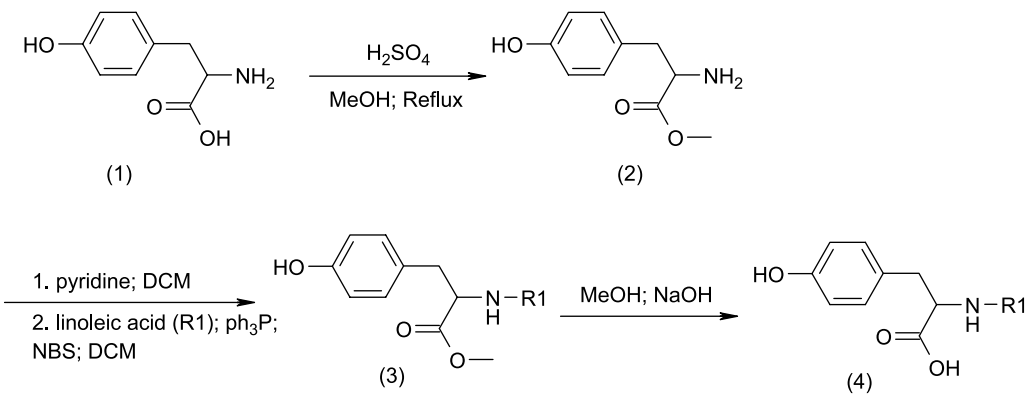

Figure 1. The synthesis of *N*-LT. Tyrosine (1), tyrosine methyl ester (2), *N*-linoleoyl tyrosine methyl ester (3), *N*-linoleoyl tyrosine (*N*-LT), (4). MeOH = methanol; DCM = dichloromethane; ph_3P = triphenylphosphine; NBS = *N*-bromosuccinimide; R1 = linoleic acid.

N-*LT (4)*. A solution of 10 ml NaOH (10%) in water was added to *N*-LT methyl ester (3) (1 g, 2.18 mmol). The mixture was stirred overnight at room temperature and then the pH was adjusted to 3 with 40% H_3PO_4. Ethyl acetate was added and the organic layer was separated and evaporated to give a colorless oil (0.95 g, 2.14 mmol) at a yield of 99%. The product showed one peak at 10.71 min (HPLC) and was identified by MS (direct injection, ES^- 442.6), ^{1}H-NMR ($CDCl_3$, 200 mHz) δ_{ppm}; 7.17(d, 2H); 6.65(d, 2H); 6.22(d, 1H); 5.31(m, 4H); 4.8(q, 1H); 3.02(d, 2H); 2.73(t, 2H); 2.16(t, 2H); 2.03(m, 6H); 1.23(s, 14H); 0.85(t; 3H). IR (net) ν_{max} 3341, 2926, 1723, 1650, 1516, 1445.

*Synthesis of 3-nitro- and 3-chloro-*N-*LT for use as standards*

N-Linoleoyl 3-nitro-tyrosine (*N*-LT(NO_2)) and *N*-linoleoyl 3-chloro-tyrosine (*N*-LT(Cl)) were synthesized in the same way as for *N*-LT, from 3-nitrotyrosine or 3-chlorotyrosine as the starting materials, respectively. Both compounds were used as standards and their stability was examined *in vitro*.

N-*LT hydrolysis and recovery from cells*

The possible degradation of *N*-LT *in vitro* and in cells was tested using two experimental approaches:

(1) *N*-LT hydrolysis was carried out with proteinase K (6 mg/ml) in Tris buffer (pH 8) at 37°C with continuous stirring. After 3 and 24 h, the formation of Tyr/LA and the disappearance of *N*-LT were monitored by HPLC, which yielded no change in *N*-LT level.
(2) Recovery of *N*-LT incubated in cells for 3 h at 37°C under the conditions described in the oxidation of *N*-LT in cells section was detected, with recovery of *N*-LT and Ox-*N*-LT from the membrane and cytosol amounting to 84%.

N-*LT distribution and cytotoxicity in cells*

A J-774 A.1 murine macrophage-like cell line was cultured at a concentration of 1.5×10^6 cells/ml in DMEM containing 5% FCS, 100,000 U/l penicillin, 100 mg/l streptomycin and 2 mM glutamine. The cell suspension was dispensed into a six-well plate and pre-incubated in a humidified incubator (5% CO_2, 95% air) at 37°C for 24 h. After 1 day, the medium was changed to HBSS and the cells were supplemented with 40 μM *N*-LT dissolved in DMSO and incubated at 37°C. After 3 h, the medium was collected and the cells were washed with 0.5 ml PBS. Membrane and cytosol fractions were separated as described elsewhere [20]. Cells were washed twice with cold PBS and scraped into 10 ml of relaxation buffer (100 mM KCl, 3 mM NaCl, 3.5 mM $MgCl_2$, 1.25 mM EGTA, 1 mM ATP, 10 mM Hepes, pH 7.4) containing 1 mM phenylmethanesulfonyl fluoride (PMSF) and 100 μM leupeptin at 4°C. Sonication for 20 s on ice yielded about 95% cell breakage. Nuclei, granules and unbroken cells were removed by centrifugation (2 min, 15,600*g*, 4°C). The supernatant was centrifuged in a Beckman Airfuge (30 min, 134,000*g*) to obtain a cell-membrane pellet and a cytosolic supernatant. Membranes and cytosolic fractions were extracted in a hexane:isopropanol solution (3:2, v/v), followed by acidification with H_2SO_4 in double-distilled water (DDW) (1:2000) to pH 3. *N*-LT concentration was determined by LC/MS/MS. Cytotoxicity was measured using the XTT method, as described: A J-774 A.1 murine macrophage-like cell line was cultured at a concentration of 0.5×10^6 cells/ml in DMEM containing 5% FCS, 100,000 U/l penicillin, 100 mg/l streptomycin and 2 mM glutamine (growth medium). The cell suspension was dispensed into a 96-well plate and pre-incubated in a humidified incubator (5% CO_2, 95% air) at 37°C for 24 h. After 1 day, the medium was changed to HBSS and the cells were supplemented with 40 μM *N*-LT dissolved in DMSO

or DMSO (0.4%) and incubated at 37°C. After 3 h incubation, medium was collected and the cells were washed with 0.2 ml HBSS. Reconstituted XTT in HBSS (1 mg/ml) was added to the wells in an amount equal to 20% of the culture medium. After 2 h incubation at 37°C, cell viability was determined at 450 nm in an ELISA reader (enzyme-linked immunoadsorbent assay, Sunrise TECAN). Cells incubated with growth medium were used as controls.

Separation of N-*LT-oxidized products by LC/MS/MS*

The LC/MS was equipped with an HPLC (Waters 2790) and a Waters photodiode array detector (model 996) connected to a MS (micromass Quattro ultima MS, UK). The HPLC column was a 3.5-μm C18 ODS XTerra (Waters) and the eluents were a gradient of solution A (0.1% acetic acid in acetonitrile) and solution B (0.1% acetic acid in DDW) as follows: Starting with 40% A; changing to 60% A for 2 min; and then to 80% A for 10 min. Finally, the column was washed with a solution of 98% A.

MS/MS analysis of the oxidized products was performed in scan mode using electron spray negative ions (ES^-). The source temperature of the MS was set at 150°C, with a cone gas flow of 75 l/h and a desolvation gas flow of 600 l/h. Peak spectra were monitored between 30 and 600 m/z and continuum data was acquired. Collision-induced dissociation MS was performed, using a collision energy of 25–30 eV and 3–3.5 kV capillary voltage. Multiple-reaction-monitoring (MRM) was performed under the same conditions. A calibration curve of *N*-LT was run in each experimental analysis.

Oxidation of N-*LT in a cell-free system*

Oxidation of *N*-LT (40 μM) with HOCl (0.1, 0.2 mM), SIN-1 (0.1 mM) or copper ions ($CuSO_4$, 20 μM) was carried out in HBSS at 37°C under continuous stirring. After 30 min, 1 or 10 h, respectively, the solutions were extracted with hexane:isopropanol (3:2) followed by acidification with a solution of DDW/H_2SO_4 to pH 3–4. The organic layer was then dried (anhydrous sodium sulfate), filtered, evaporated to dryness in an evaporator, and resuspended in acetonitrile (HPLC-grade) for LC/MS/MS analysis.

For treatment with HOCl, a stock solution of NaOCl was prepared, and the concentration was determined spectrophotometrically ($\varepsilon_{292} = 350\,M^{-1}\,cm^{-1}$). When copper ions were used as the inducer, a fresh stock solution of $CuSO_4$ was prepared before each experiment. For treatment with SIN-1, a stock solution of SIN-1 was prepared in 1 N NaOH.

Oxidation of N-*LT in cells*

J-774 A.1 murine macrophage-like cells were cultured at a concentration of 1.5×10^6 cells/ml in DMEM containing 5% FCS, 100,000 U/l penicillin, 100 mg/l streptomycin and 2 mmol/l glutamine. The cell suspension was dispensed into a six-well plate and pre-incubated in a humidified incubator (5% CO_2, 95% air) at 37°C for 24 h. After 1 day, the medium was changed to HBSS. The cells were supplemented with 40 μM *N*-LT dissolved in DMSO (4 μl in 1 ml HBSS) and incubated at 37°C. Control cells were supplemented with DMSO (0.4%) with no addition of *N*-LT. After 3 h, the medium was removed and the cells were washed with 0.5 ml HBSS prior to the following treatments.

Copper ion-induced macrophages. Twenty micromole $CuSO_4$ dissolved in HBSS was added to J-774 macrophages. After 10 h of incubation, the cells were washed twice with 0.5 ml HBSS, harvested and extracted twice with hexane–isopropanol (3:2) followed by acidification with H_2SO_4 in DDW to pH 3. The samples were then dried and evaporated, and resuspended in acetonitrile for LC/MS analysis.

HOCl-induced monocytes. HOCl dissolved in HBSS (0.2 and 2 mM) was added to PLB-985 pre-monocytes. These were incubated and treated as described for J-774 A.1 cells. After 30 min of incubation, the cells were washed twice with 0.5 ml HBSS, harvested, extracted, dried and resuspended with acetonitrile for LC/MS analysis.

SIN-1-induced macrophages. SIN-1 dissolved in HBSS (0.1 mM) was added to the J-774 cells. After 30 min of incubation, the cells were washed twice with 0.5 ml HBSS, harvested, extracted, dried and resuspended with acetonitrile for LC/MS analysis. Cells containing *N*-LT (40 μM) without oxidants were used as controls.

Mouse peritoneal macrophages (MPM)

Apolipoprotein-deficient (E^0) mice were generously provided by Dr Jan Breslow (Rockefeller University, New York). Gene-targeting in mouse embryonic stem cells was used to create these mice, which lack apolipoprotein E and are characterized by hypercholesterolemia, oxidative stress and accelerated atherosclerosis [21]. These mice were compared with BalbC mice (as controls) of the same age, sex and genetic background.

MPMs were harvested from 2- and 4-month-old BalbC and E^0 mice 3 days after intraperitoneal

injection of 3 ml 4% thioglycolate. The cells were washed twice with PBS, resuspended at a concentration of 3×10^6 cells/ml in DMEM containing 10% FCS, 100,000 U/l penicillin, 100 mg/l streptomycin and 2 mM glutamine. The cell suspension was dispensed into a six-well plate and incubated in a humidified incubator (5% CO_2, 95% air) at 37°C for 4 h. The dishes were washed once with 5 ml DMEM to remove nonadherent cells. The monolayer was then incubated with 40 or 80 μM *N*-LT under similar conditions. After 20 h, the medium was removed and the cells were harvested and extracted twice with hexane–isopropanol (3:2) followed by acidification with H_2SO_4 in DDW to pH 3. The samples were then dried and evaporated, and resuspended in acetonitrile for LC/MS analysis.

Statistical analysis

The relative amounts of the oxidation products were calculated as μM percentage of the unoxidized *N*-LT in the sample. Each experiment was repeated at least three times and Student's *t*-test was used to analyze the significance of the results, which are given as means ± SE.

Results

N-LT was synthesized from Tyr and LA by first protecting the Tyr carboxylic group (by making methyl ester), then coupling the protected Tyr with LA, forming an amide bond, and finally, hydrolyzing the methyl ester to yield *N*-LT. This synthetic *N*-LT was then used throughout the study (Figure 1).

Analysis of the cellular distribution of *N*-LT in the medium, membrane and cytosol revealed that 16% of the total *N*-LT remains in the media, while most of the *N*-LT (80% of the total incubated) is trapped in the macrophage membrane and 4% is found in the cytosol.

Cytotoxicity measurements revealed no damage to the viability of cells incubated with HBSS or with *N*-LT for 3 h relative to those incubated with growth medium.

HOCl-induced oxidation of N-*LT in the cell-free system and in cell culture*

Treatment of *N*-LT (40 μM) in a cell-free system with HOCl (0.2 mM) resulted in the formation of a major product (*N*-L(HOCl)T) obtained from the addition of one equivalent of HOCl to one of the two LA double bonds (10.8%, representing 77% of the total Ox-*N*-LT detected) (Figure 2). Another product was *N*-linoleoyl 3-chloro-tyrosine (*N*-LT(Cl)), resulting from chlorination on the Tyr aromatic ring (1.5%). A minor product (0.2%) was obtained as a result of two equivalents of HOCl added to the LA moiety (*N*-L(diHOCl)T). An oxidative product containing epoxide on the LA of the *N*-LT was found, with or without added oxidant, in similar amounts (1.3%), suggesting that the epoxide product at the detected level could be formed in all cases under the experimental conditions (Figure 2). Upon increasing the HOCl concentration to 0.4 mM, a parallel increase in the total amount of Ox-*N*-LT was noted, from 14 to 29% (of the total *N*-LT added), with the major Ox-*N*-LT products being *N*-L(HOCl)T (up to 20%), *N*-LT(Cl) (up to 4.3%) and *N*-L(diHOCl)T (up to 2%) (data not shown).

We next studied the oxidation of *N*-LT in a cell system of J-774 A.1 macrophages. Incubation of *N*-LT (40 μM) with the cells, followed by cell oxidation with HOCl (0.2 mM) for 30 min and then extraction of the oxidized materials and their analysis by LC/MS/MS, showed an increase in the amount of total Ox-*N*-LT in the cells, although this amount was still lower by 2.3-fold than the level of Ox-*N*-LT formed in the cell-free system. The predominant *N*-L(HOCl)T was obtained under cell-free conditions with a minor level of two other Ox-*N*-LT products, i.e. *N*-L(epoxy)T and *N*-L(epoxy-diol)T, where the second double bond of the LA was reacted to form diol. The formation of the last product is not necessarily linked to the addition of HOCl.

The Ox-*N*-LT products were identified by either synthesizing them (3-chloro-*N*-LT, 3,5-dichloro-*N*-LT), or deducing them from their MS spectra in scan mode using electrospray negative ions (ES^-), as well as from fragmentation of the molecular ions, using daughter ion and/or MRM methods.

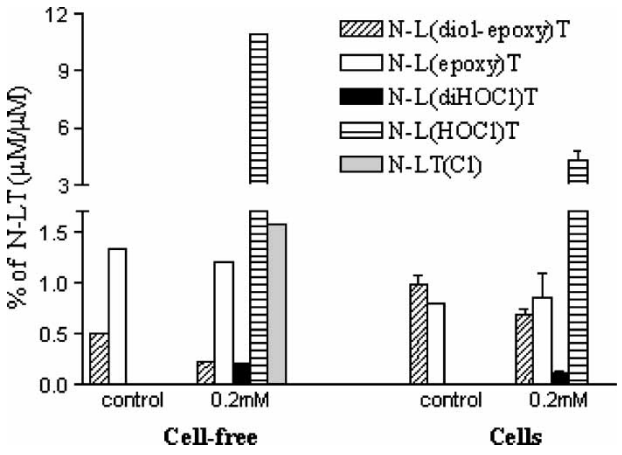

Figure 2. Oxidized products from HOCl-induced *N*-LT oxidation in the cell-free system and in cells. *N*-LT (40 μM) in HBSS was incubated with PLB-985 pre-monocytes cells for 3 h and then HOCl was added (0.2 mM). After 30 min, the cells were extracted and the organic phase was analyzed by LC/MS/MS. The effect of HOCl on the oxidation of *N*-LT in the cell-free system was studied under similar conditions.

Thus, the LC/MS/MS analysis of HOCl-induced oxidation of *N*-LT in cells and *in vitro* (Figure 3) revealed four identified compounds: Compound 3A (*N*-L(epoxy-diol)T) with a molecular ion of *m/z* 492 (M^{-1}) and a major fragmentation of *m/z* 180, corresponding to Tyr (M^{-1}-LA); 3-chloro *N*-LT (3B, *N*-LT(Cl)), in which chlorination of the Tyr aromatic ring occurs, with a molecular mass of *m/z* 476.8/478.8 ($^{35}M^{-1}/^{37}M^{-1}$) (ms scan) and major fragmentations (daughter scan) at *m/z* 432 (M^{-1}-CO_2) and *m/z* 214 (corresponding to chloro-Tyr) (Figure 3B); *N*-L(HOCl)T (molecular mass of *m/z* 494.6/496.6 ($^{35}M^{-1}/^{37}M^{-1}$)), formed by the addition of HOCl to the LA moiety, with fragmentation of *m/z* 458 (daughter ion of M^{-1}-HCl resulting from the molecular of *m/z* 494.6), *m/z* 397 (fragmentation between C_{11} and C_{12}) and fragmentation at *m/z* 180 (Figure 3C); and finally, *N*-L(diHOCl)T, with a molecular mass of *m/z* 546.6/548.6 ($^{35}M^{-1}/^{37}M^{-1}$) (ms scan) and fragmentation ions at *m/z* 510 (M^{-1}-HCl), *m/z* 474 (M^{-1}-2HCl) and *m/z* 180 as detected by daughter scan (Figure 3D).

The oxidative effect of copper ions on N-*LT in the cell-free system and in cell culture*

Upon exposure of *N*-LT to copper ions (20 μM) for 10 h in a cell-free system, only two major Ox-*N*-LT products were obtained: *N*-L(epoxy)T (2.3% ± 0.19) and *N*-LT-hydroperoxide (*N*-L(OOH)T, 0.42% ± 0.03). Both compounds were also present in the control, where no copper ions had been added (Figure 4), indicating that these types of oxidation can occur even when samples of *N*-LT are in a solution that is open to air. In similar experiment in cells (J-774 A.1 macrophages), the amount of *N*-L(epoxy)T was about threefold less than its amount in the cell-free system (1.8% ± 0.02 in the cell-free system vs. 0.6% ± 0.15 in cells, $p < 0.05$). Addition of copper ions to the cells did not affect the amount of *N*-L(epoxy)T formed (0.67% ± 0.07). The level of *N*-L(OOH)T detected in the cells was also less than that seen in the cell-free experiment (0.03 and 0.15%, respectively), but it increased significantly upon addition of copper ions to the cells

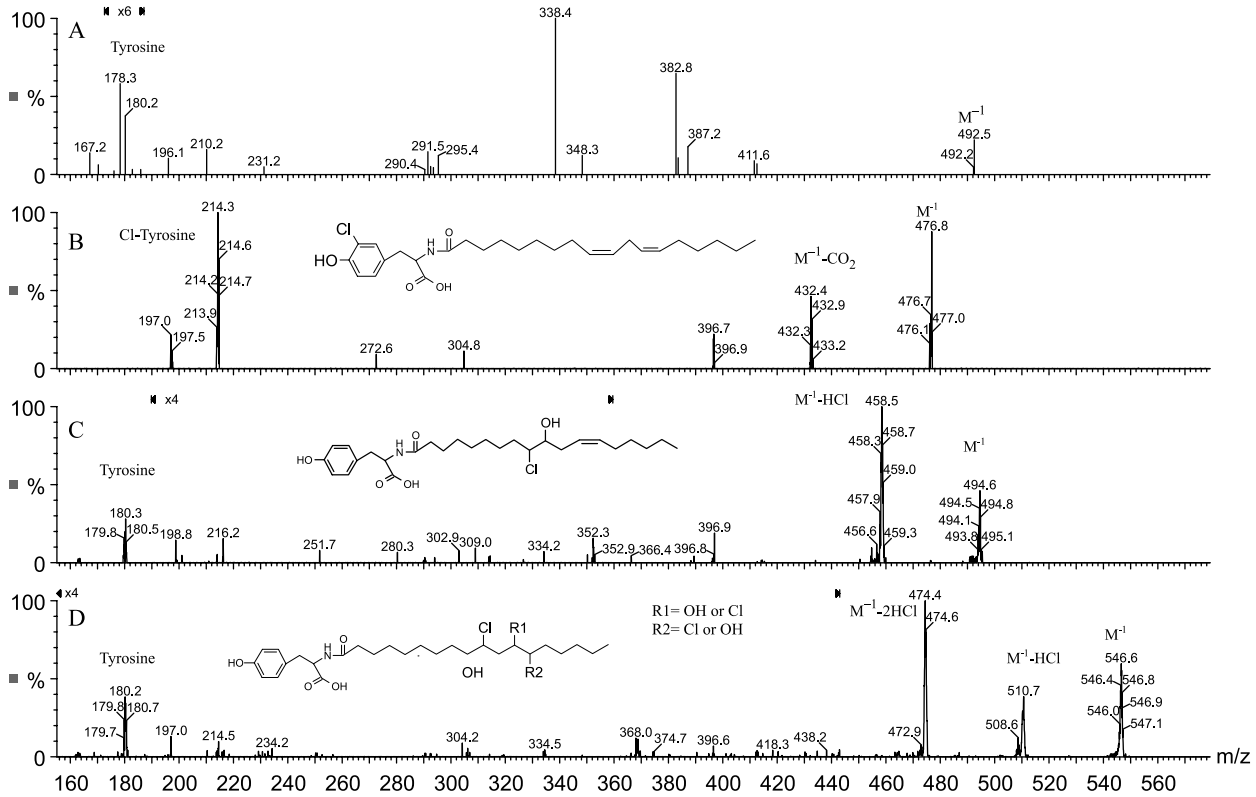

Figure 3. LC/MS/MS analysis of the products of the HOCl-induced oxidation of *N*-LT. *N*-LT was treated with HOCl as described in "Materials and Methods" section. The organic extract from the reaction mixture was analyzed qualitatively and quantitatively by LC/MS/MS using LC (HP-1100) and an RP-8 column with acetonitrile: Water as the eluents and with a diode-array detector as an additional detector. Compounds A–D was identified using scan mode and the molecular ions were further fragmented by collision-induced dissociation MS using 25–30 collision energy and 3–3.5 capillary voltage. (A) *N*-LT-dihydroxy-epoxy (*N*-L(diol-epoxy)T, $M^{-1} = 492$) and its fragmentation ions at *m/z* 180 (tyrosine); (B) *N*-LT(Cl) ($M^{-1} = 476$) and its fragmentation ions at *m/z* 432 (M^{-1}-CO_2) and *m/z* 214 (*Cl*-tyrosine); (C) *N*-linoleoyl tyrosine-HOCl (*N*-L(HOCl)T, $M^{-1} = 494$) and its fragmentation ions at *m/z* 458 (M^{-1}-HCl), *m/z* 397 (fragmentation between C_{11} and C_{12}) and *m/z* 180; (D) *N*-L(diHOCl)T ($M^{-1} = 546$) and its fragmentation ions at *m/z* 510 (M^{-1}-HCl), *m/z* 474 (M^{-1}-2HCl) and fragmentation at *m/z* 180.

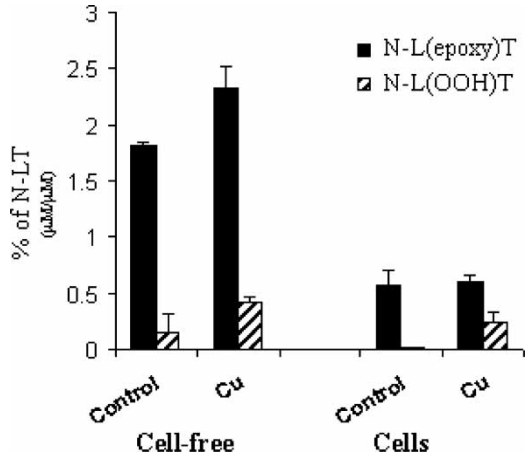

Figure 4. Oxidized products from copper ion-induced *N*-LT oxidation in a cell-free system and in J-774 cells. Cells were incubated with copper ions (20 μM) and *N*-LT (40 μM). After 10 h, the cells were extracted and the organic phase was analyzed in LC/MS/MS. The effect of copper ions on the oxidation of *N*-LT in a cell-free system was studied under the same conditions.

(from 0.03 ± 0.001 to $0.30 \pm 0.07\%$, $p < 0.05$). Figure 5 shows the LC/MS/MS of *N*-L(epoxy)T with a molecular ion of *m/z* 458 (M^{-1}) and major fragmentations at *m/z* 372 (M^{-1}-C_6H_{14}) and *m/z* 180. The spectrum of *N*-L(OOH)T gives the major daughter fragment at an *m/z* of 388 (M^{-1}-C_6H_{14}), resulting from a molecular ion of *m/z* 474 and Tyr peak (*m/z* 180), showing that the Tyr aromatic ring remained unaffected.

SIN-1 induced oxidation of N-*LT in the cell-free system and in cell culture*

Treatment of *N*-LT (40 μM) in the cell-free system with 0.1 or 1.0 mM SIN-1 yielded one major Ox-*N*-LT product (Figure 6), from mono-nitration of the Tyr aromatic ring (*N*-LT(NO_2), $7.0 \pm 0.2\%$ and $21.2 \pm 2.5\%$ Ox-*N*-LT/total *N*-LT, obtained with 0.1 and 1.0 mM SIN-1, respectively. In addition, a minor Ox-*N*-LT product was formed where the LA moiety was oxidized to hydroperoxide (*N*-L(OOH)T), with the OOH connected to carbon 13 ($1.8 \pm 0.7\%$ *N*-L(OOH)T/total *N*-LT, using 1 mM SIN-1). As shown with the other oxidants, epoxidation of LA took place independently of the presence or type of oxidant used. Addition of SIN-1 to J-774 A.1 cells, as previously seen for HOCl and copper ions, increases the amount of total Ox-*N*-LT, although the increase was less pronounced than in the cell-free system (10.7 ± 0.4 vs. $1.865 \pm 0.1\%$, using 0.1 mM SIN-1, and 25.05 ± 1.9 vs. $11.25 \pm 1.5\%$ using 1.0 mM SIN-1, respectively, $p < 0.05$). In parallel, the amount of epoxide detected in cells diminished significantly (from 2.1 ± 0.1 to $0.3 \pm 0.07\%$ in the cell-free system and control cells without oxidant,

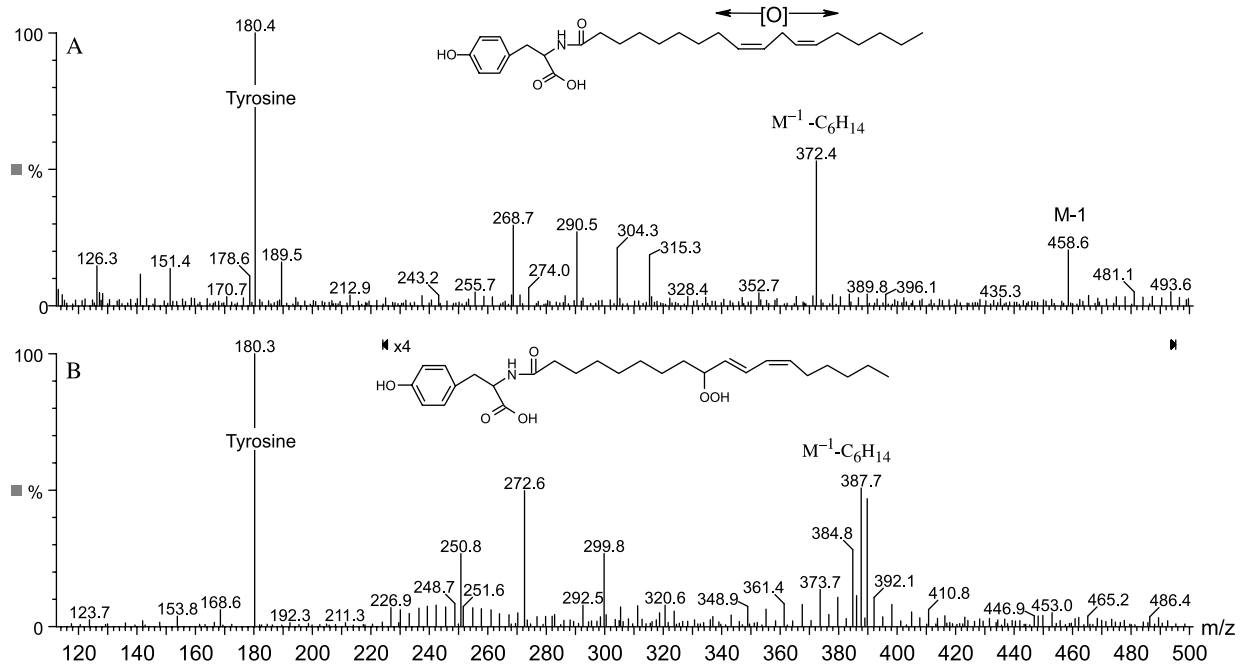

Figure 5. LC/MS/MS analysis of the products from copper ion-induced oxidation of *N*-LT. *N*-LT (40 μM) was induced by copper ions ($CuSO_4$, 20 μM) as described in "Materials and Methods" section. The organic extract from the reaction mixture was analyzed qualitatively and quantitatively by LC/MS/MS using LC (HP-1100) and an RP-8 column with acetonitrile: Water as the eluents and additionally, with a diode-array detector. Compounds A and B were identified using scan mode and the molecular ions were further fragmented by collision-induced dissociation MS using 25–30 collision energy and 3–3.5 capillary voltage. (A) *N*-L(epoxy)T (*N*-L(epoxy)T, $M^{-1} = 458$) and its fragmentation ions: *m/z* 372 (M^{-1}-C_6H_{14}) and *m/z* 180 (tyrosine); (B) *N*-LT-hydroperoxide with fragments at *m/z* 388 (M^{-1}-C_6H_{14}) and *m/z* 180 resulting from molecular ions at *m/z* 474 (*N*-L(OOH)T).

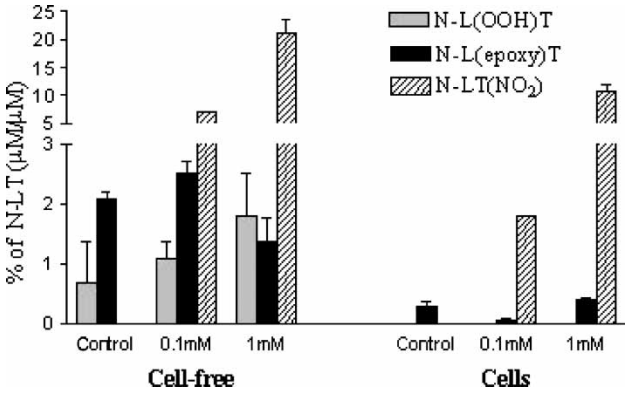

Figure 6. Oxidized products from SIN-1-induced *N*-LT oxidation in cell culture. *N*-LT (40 μM) in HBSS was incubated with J-774 cells for 3 h prior to the addition of SIN-1 (0.1 mM). After 1 h, the cells were extracted and the organic phase was analyzed in LC/MS/MS. The effect of SIN-1 on the oxidation of *N*-LT in the cell-free system was studied under similar conditions.

respectively, $p < 0.05$) and no *N*-L(OOH)T could be detected. Ox-*N*-LT products were identified using the same analytical techniques as with the other inducers, i.e. by comparison with standard (*N*-LT(NO_2)) and from LC/MS/MS analysis. Results are shown in Figure 7, presenting the MS spectrum of *N*-LT (Figure 7A) and the spectrum of *N*-L(epoxy)T (Figure 7B). The spectrum of the major Ox-*N*-LT (*N*-LT(NO_2)) is shown in Figure 7C with nitro groups on the aromatic ring, with a molecular mass of *m/z* 487 (M^{-1}) and major fragmentations at *m/z* 443 (M^{-1}-CO_2), and *m/z* 225 (nitro-Tyr). The MS spectra of the *N*-L(OOH)T are shown in Figure 7D with a molecular mass of *m/z* 474 (M^{-1}) and an -OOH group on carbon 13, as evidenced by its fragmentation between C_{11} and C_{12} at *m/z* 346 (M^{-1}-$C_7H_{14}O_2$) and the Tyr peak (*m/z* 180).

The effect of mouse peritoneal macrophages on N-*LT oxidation*

MPM harvested from BalbC and E^0 mice (at both 2 and 4 months of age) after induction of inflammatory conditions (thioglycolate injection) were used to test whether activated macrophages can induce oxidation of the *N*-LT marker. The results are summarized in Figure 8, demonstrating the detection of *N*-L(epoxy)T and *N*-L(OOH)T, the LA moiety having been oxidized to epoxide or to hydroperoxide, respectively. Figure 8 also shows that epoxidation of the LA took place in both types of mice, BalbC and E^0, and that the level was not significantly different (1.68 ± 0.24 vs. 2.4 ± 0.45 μM/μM *N*-LT, respectively). The level of epoxidation of the LA moiety of the marker as a result of its incubation with macrophages

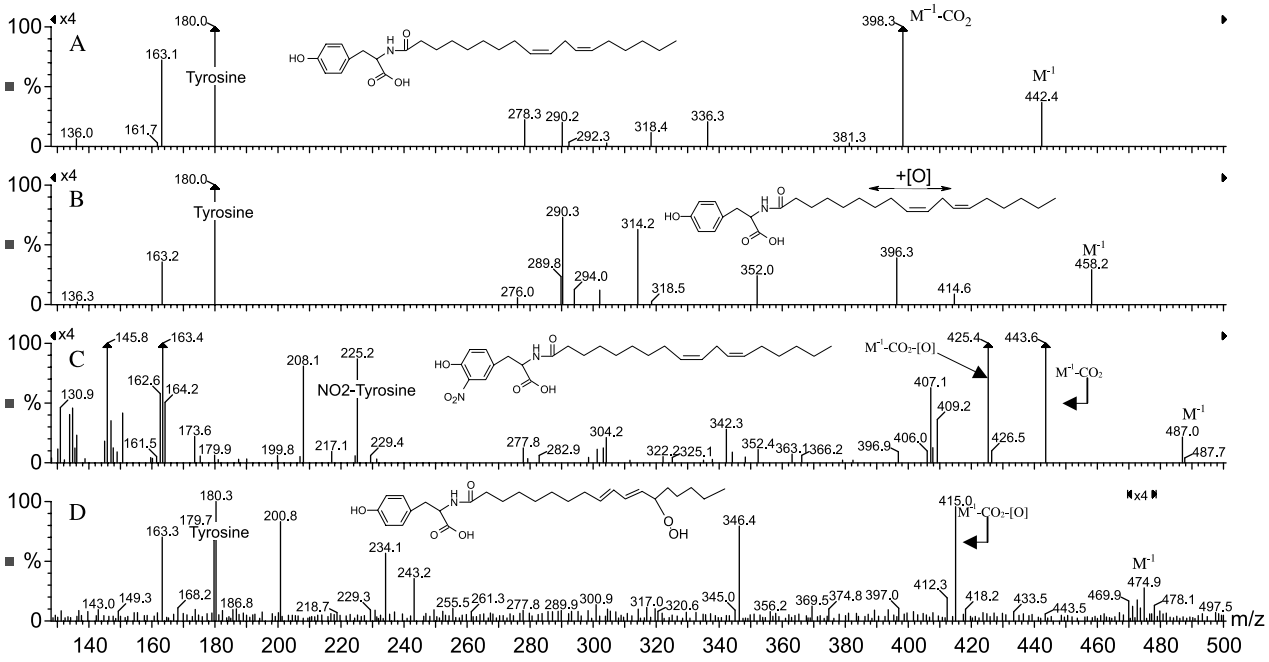

Figure 7. LC/MS/MS analysis of the products from SIN-1-induced oxidation of *N*-LT. *N*-LT was induced by SIN-1 as described in "Materials and Methods" section. The organic extract from the reaction mixture was analyzed qualitatively and quantitatively by LC/MS/MS using LC (HP-1100) and an RP-8 column with acetonitrile: Water as the eluents, and additionally, with a diode-array detector. Compounds A–D were identified using scan mode and the molecular ions were further fragmented by collision-induced dissociation MS using 25–30 collision energy and 3–3.5 capillary voltage. (A) *N*-LT ($M^{-1} = 442$) and its fragmentation ions at *m/z* 398 (M^{-1}-CO_2) and *m/z* 180 (tyrosine); (B) *N*-L(epoxy)T ($M^{-1} = 458$) and its fragmentation ion at *m/z*180; (C) *N*-LT(NO2) ($M^{-1} = 487$) and its fragmentation ions at *m/z* 425 (M^{-1}-CO_2) and 225 (3-nitro-tyrosine). (D) *N*-L(OOH)T ($M^{-1} = 474$) and its fragmentation ions at *m/z* 346 (M^{-1}-$C_7H_{14}O_2$) and the tyrosine peak (*m/z* 180).

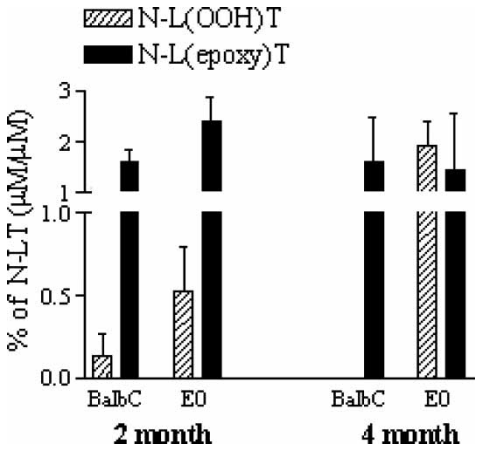

Figure 8. Mouse peritoneal macrophage-induced *N*-LT oxidation. Mouse peritoneal macrophages were harvested from BalbC and E^0 mice 3 days after intraperitoneal injection of 3 ml 4% thioglycolate. The cells were washed and incubated for 4 h as described in materials and methods. Cells were then incubated with 40 μM *N*-LT. After 20 h, the medium was removed and the cells were harvested, extracted and injected into LC/MS.

from BalbC or E^0 mice was also not significant at 4 months of age (1.61 ± 0.87 vs. 1.45 ± 1.10 μM/μM *N*-LT, respectively), or between 2- vs. 4-month-old mice. The amount of *N*-LT-hydroperoxide (*N*-L(OOH)T) at 2 months of age was 0.13 ± 0.13 vs. 0.52 ± 0.27 μM/μM *N*-LT, in BalbC vs. E^0 mice, respectively, and much more pronounced at 4 months of age (below the limit of detection vs. 1.93 ± 0.45 μM/μM *N*-LT, respectively). Moreover, with progression of the atherogenic condition (from 2 to 4 months of age), a significant elevation in the *N*-L(OOH)T level was anticipated in the E^0 mice (0.52 ± 0.27 vs. 1.93 ± 0.45, respectively, $p < 0.05$).

Discussion

We have recently shown that exposure of Tyr, LA and cholesterol, alone or in a mixture, to different types of oxidants results in the formation of different types of oxidative products [22]. In the present study, we expanded that research by designing an exogenous marker for oxidative stress constructed from Tyr and LA (connected by covalent bond). We hypothesized that such a marker could be used to characterize pathological conditions associated with oxidative stress, based on the type of Ox-*N*-LT products formed.

The idea was that this new marker's presence in an organism could be distinguished from the endogenous elements constructing it. Any alterations that might occur to it during its incubation with the investigated system (such as macrophages, blood, tissue, organs) could then be attributed to the influence of that system on the marker. Tyr and LA were selected to construct the marker because both are sensitive to ROS/RNS and have been extensively investigated for their reaction products with oxidants [23–28]. Furthermore, each represents a major family of the body's building blocks: the proteins and unsaturated fatty acids, respectively. After combining them into one molecule (*N*-LT), their active sites, i.e. the aromatic ring on the Tyr and the two double bonds on the LA, remained intact. Oxidation of each of the *N*-LT subunits can thus be distinguished from any other oxidized endogenous biomolecules present in the tested sample. In addition, the strong amide bond connecting the Tyr and the LA is not likely to be easily hydrolyzed chemically or enzymatically by proteases. Phagocytes, such as monocytes and macrophages, are an important source of highly reactive oxidants, generating HOCl from H_2O_2 and chloride, and $ONOO^-$ from nitric oxide and $O_2^{-\cdot}$. Exposure of LDL to HOCl results in the chlorination and oxidation of their protein and lipid constituents, causing LDL aggregation, and increased cellular uptake by macrophages [9,29]. In a recent study, exposure of LDL to human monocytes resulted in LDL lipid peroxidation and protein nitration. Moreover, myeloperoxidase (MPO), known to generate RNS when incubated with LDL, resulted in increased LDL uptake by macrophages and foam-cell formation [30].

In the present study, the effect of HOCl-induced *N*-LT oxidation differed significantly when the *N*-LT was incubated with macrophages, relative to direct treatment of *N*-LT with HOCl. The oxidation of *N*-LT was significantly retarded in the cell system, by 57%, and unlike the cell-free system, no *N*-LT(Cl) was detected (Figure 2). These results could be explained by the cells' buffering effect on the extent of *N*-LT oxidation in general, due to either its reductant content (low- and high-molecular-weight antioxidants) or the presence of other substances which could compete with *N*-LT for the HOCl, thereby reducing its availability to the former. In addition, as the pattern of oxidation and the nature of the ROS are strongly dependent on the cellular environment and can be modified from one system to the next, different oxidation patterns can result between the cells and the cell-free system. Another important finding was the selectivity of the reactions in the cells: Under our experimental conditions, only the unsaturated fatty acid reacted, but not the Tyr (no 3-chloro-Tyr formed) and thus, under the experimental conditions in cells, LA was the favored molecule for reactions with HOCl.

Copper (II) ions are widely used to initiate lipid peroxidation in model systems, particularly in studies of LDL oxidation [31–35]. Copper (II) ions can induce lipid peroxidation in the absence of an additional reducing agent, and it has often been assumed that this involves the reduction of copper (II) by a pre-formed lipid hydroperoxide, resulting in the

generation of a peroxyl radical ($ROO^{\cdot}$), which may then initiate further cycles of peroxidation [36].

Incubation of *N*-LT with cells followed by their oxidation with copper ions, and a comparison of the results to similar experiments in the cell-free system, revealed that cells buffer the effects of oxidants such as HOCl and copper ions. The present results show that *N*-LT-epoxide is formed in relatively large amounts in the cell-free system, but its formation is not associated with the presence of oxidant (1.8% in the control and 2.3% in the presence of copper ions). In cells, however, the amount of epoxidation diminishes considerably (0.6%) and again, this amount is not related to the presence or absence of copper ions. Exposing LA to air is sufficient to oxidize part of it to linoleoyl hydroperoxide (L-OOH), a reaction which is accelerated in the presence of copper ions. The present study shows that *N*-LT in cells does not oxidize to *N*-L(OOH)T, despite exposure of the cells to air for 10 h, and no *N*-L(OOH)T was detected in the controls (no oxidant); on the other hand, the addition of copper ions resulted in *N*-L(OOH)T formation in the cell system. These experiments indicate that in addition to the buffering effect of the cells, the copper ions, under our experimental conditions, oxidize LA but do not affect Tyr.

RNS derived from NO can be strong oxidants, which can oxidize lipids, proteins and DNA and they are formed *in vivo* under pathological conditions such as inflammation [37] and atherosclerosis [38]. SIN-1 at physiological pH decomposes to form nitric oxide and $O_2^{-\cdot}$ [39] and these can react with each other to form a powerful oxidant, $ONOO^-$. In the present study, using the exogenous marker *N*-LT, the effect of SIN-1 in cells was tested and the results compared with its effects in a cell-free system. Similar to the two previous inducers tested, HOCl and copper ions, the amount of SIN-1-induced *N*-LT oxidation in cells was significantly lower (3.9–1.9 times) than the Ox-*N*-LT formed in the cell-free system. These observations were similar to the results obtained from both previous oxidants. Furthermore, SIN-1 decomposes to $O_2^{-\cdot}$, which can be removed by the cell's SOD ($O_2^{-\cdot}$ dismutase) and thus, decreases the amount of $ONOO^-$ formation. Another important finding of the present study is that using the designed marker, one may be able to identify the type of oxidant (ROS/RNS) affecting the cells at any given time, based on the type of Ox-*N*-LT products formed after incubating *N*-LT with the cells. Thus, exposing cells to HOCl or copper ions resulted in exclusive attack on the LA residue of the *N*-LT. With HOCl, an additional reaction to the LA double bond (*N*-L(HOCl)T) was preferred and with copper ions, the formation of a linoleoyl hydroperoxide residue (*N*-L(OOH)T) was favored. In contrast, when RNS (SIN-1) was the inducer, the Tyr moiety of *N*-LT was most reactive, with predominantly a nitration reaction occurring on the Tyr aromatic ring and formation of *N*-LT(NO_2). This observed selectivity of *N*-LT's reaction with different ROS/RNS requires further investigation.

MPM from atherosclerotic E^0 mice are known to produce ROS/RNS at an increased rate relative to BalbC control mice, as evidenced by enhanced plasma lipoprotein oxidation [40], and by the accumulation of oxysterols and lipid peroxides in their macrophages [41–43]. MPM from atherosclerotic or control mice were incubated with *N*-LT to determine whether the cells can oxidize the *N*-LT with no addition of any exogenous oxidants, and if the *N*-LT marker can distinguish between the two types of cells, which may differ in their ability to increase activation and ongoing production of ROS/RNS. Our results indicated that the *N*-LT is sufficiently sensitive to relay this information. *N*-LT was oxidized by both cell types, but MPM from 2-month-old E^0 were shown to produce four times more *N*-L(OOH)T than the control cells (MPM from BalbC) (0.52 vs. 0.13%, but still not significant, Figure 8). Moreover, the type of oxidative products formed, at least initially, clearly originated from the peroxidation reactions [33,44]. The amount of *N*-LT-epoxide detected was not significant, in agreement with our finding that LA can be oxidized to epoxide, even in a solution that is open to air. When macrophages from 4-month-old E^0 mice were tested for their Ox-*N*-LT content (older E^0 mice are expected to be more atherosclerotic), the differences in the amount of *N*-L(OOH)T between BalbC and E^0 mice were significantly more pronounced. Thus, *N*-L(OOH)T could not be seen in the MPM in control BalbC mice, whereas 1.94% *N*-L(OOH)T was observed in the MPM from E^0 mice; on the other hand, the level of *N*-L(epoxy)T did not increase. In MPM from both mice, *N*-L(HOCl)T was detected in about similar amounts (0.1% μM).

It may be concluded that while epoxidation of LA (formation of *N*-LT-epoxide) is a process not necessarily related to *in vivo* oxidative events, reaction of *N*-LT with HOCl to yield *N*-L(HOCl)T may be a sign of inflammation-induced oxidative stress, and detection of *N*-L(OOH)T above a certain amount may be a sign of oxidation-induced atherosclerosis. This hypothesis needs to be further investigated. Finally, the suggested marker *N*-LT, which we are currently developing further, illustrates a novel concept, which may overcome some of the drawbacks associated with the existing biomarkers.

This concept of using an exogenous marker to characterize oxidative stress in a biological system appears to be feasible and may be exploited as a fingerprint for the early identification of different oxidative-stress-related pathological conditions.

References

[1] Finkel T, Holbrook NJ. Oxidants, oxidative stress and the biology of ageing. Nature 2000;408:239–247.

[2] Halliwell B. Effect of diet on cancer development: Is oxidative DNA damage a biomarker? Free Radic Biol Med 2002; 32:968–974.

[3] Aviram M. Review of human studies on oxidative damage and antioxidant protection related to cardiovascular diseases. Free Radic Res 2000;33:S85–S97.

[4] Saran M, Beck-Speier I, Fellerhoff B, Bauer G. Phagocytic killing of microorganisms by radical processes: Consequences of the reaction of hydroxyl radicals with chloride yielding chlorine atoms. Free Radic Biol Med 1999;26:482–490.

[5] Halliwell B, Gutteridge JMC. Free radicals in biology and medicine. 3rd. ed. Oxford: Oxford University Press; 1999.

[6] Berliner LJ, Khramtsov V, Fujii H, Clanton TL. Unique *in vivo* applications of spin traps. Free Radic Biol Med 2001; 30:489–499.

[7] Utsumi H, Yamada K. *In vivo* electron spin resonance-computed tomography/nitroxyl probe technique for non-invasive analysis of oxidative injuries. Arch Biochem Biophys 2003;416:1–8.

[8] Pryor WA. Forum on oxidative stress status (OSS) and its measurement. Free Radic Biol Med 2000;29:387.

[9] Hazen SL, Heinecke JW. 3-Chlorotyrosine, a specific marker of myeloperoxidase-catalyzed oxidation, is markedly elevated in low-density lipoprotein isolated from human atherosclerotic intima. J Clin Investig 1997;99:2075–2081.

[10] Gaut JP, Byun J, Tran HD, Heinecke JW. Artifact-free quantification of free 3-chlorotyrosine, 3-bromotyrosine, and 3-nitrotyrosine in human plasma by electron capture-negative chemical ionization gas chromatography mass spectrometry and liquid chromatography-electrospray ionization tandem mass spectrometry. Anal Biochem 2002;300:252–259.

[11] Fu S, Wang H, Davies M, Dean R. Reactions of hypochlorous acid with tyrosine and peptidyl-tyrosyl residues give dichlorinated and aldehydic products in addition to 3-chlorotyrosine. J Biol Chem 2000;275:10851–10858.

[12] van Dalen CJ, Winterbourn CC, Senthilmohan R, Kettle AJ. Nitrite as a substrate and inhibitor of myeloperoxidase. Implications for nitration and hypochlorous acid production at sites of inflammation. J Biol Chem 2000; 275: 11638–11644.

[13] Woods AA, Linton SM, Davies MJ. Detection of HOCl-mediated protein oxidation products in the extracellular matrix of human atherosclerotic plaques. Biochem J 2003;370:729–735.

[14] Tallman KA, Pratt DA, Porter NA. Kinetic products of linoleate peroxidation: Rapid beta-fragmentation of non-conjugated peroxyls. J Am Chem Soc 2001;123: 11827–11828.

[15] Aviram M, Vaya J. Markers for low-density lipoprotein oxidation. Methods Enzymol 2001;335:244–256.

[16] O'Donnell VB, Freeman BA. Interactions between nitric oxide and lipid oxidation pathways: Implications for vascular disease. Circ Res 2001;88:12–21.

[17] Winterbourn CC, van den Berg JJ, Roitman E, Kuypers FA. Chlorohydrin formation from unsaturated fatty acids reacted with hypochlorous acid. Arch Biochem Biophys 1992; 296:547–555.

[18] Lima ES, Di Mascio P, Abdalla DS. Cholesteryl nitrolinoleate, a nitrated lipid present in human blood plasma and lipoproteins. J Lipid Res 2003;44:1660–1666.

[19] Froyen P. Phosphorus in organic synthesis. Acyloxyphosphonium salts as chemoselective acylating reagents. Tetrahedron Lett 1997;38:5359–5362.

[20] Nunoi H, Rotrosen D, Gallin JI, Malech HL. Two forms of autosomal chronic granulomatous disease lack distinct neutrophil cytosol factors. Science 1988;242:1298–1301.

[21] Plump AS, Smith JD, Hayek T, Aalto-Setala K, Walsh A, Verstuyft JG, Rubin EM, Breslow JL. Severe hypercholesterolemia and atherosclerosis in apolipoprotein E-deficient mice created by homologous recombination in ES cells. Cell 1992;71:343–353.

[22] Szuchman A, Aviram M, Tamir S, Vaya J. Cholesterol, linoleic acid or/and tyrosine yield different spectra of products when oxidized alone or in a mixture: Studies in various oxidative systems. Free Radic Res 2003;37:1277–1288.

[23] Aviram M, Fuhrman B. LDL oxidation by arterial wall macrophages depends on the oxidative status in the lipoprotein and in the cells: Role of prooxidants vs. antioxidants. Mol Cell Biochem 1998;188:149–159.

[24] Chapman AL, Senthilmohan R, Winterbourn CC, Kettle AJ. Comparison of mono- and dichlorinated tyrosines with carbonyls for detection of hypochlorous acid modified proteins. Arch Biochem Biophys 2000;377:95–100.

[25] Halliwell B. Lipid peroxidation, antioxidants and cardiovascular disease: How should we move forward? Cardiovasc Res 2000;47:410–418.

[26] Jerlich A, Pitt AR, Schaur RJ, Spickett CM. Pathways of phospholipid oxidation by HOCl in human LDL detected by LC-MS. Free Radic Biol Med 2000;28:673–682.

[27] Botti H, Batthyany C, Trostchansky A, Radi R, Freeman BA, Rubbo H. Peroxynitrite-mediated alpha-tocopherol oxidation in low-density lipoprotein: A mechanistic approach. Free Radic Biol Med 2004;36:152–162.

[28] Radi R. Nitric oxide, oxidants, and protein tyrosine nitration. Proc Natl Acad Sci USA 2004;101:4003–4008.

[29] Hazell LJ, van den Berg JJ, Stocker R. Oxidation of low-density lipoprotein by hypochlorite causes aggregation that is mediated by modification of lysine residues rather than lipid oxidation. Biochem J 1994;302:297–304.

[30] Heller JI, Crowley JR, Hazen SL, Salvay DM, Wagner P, Pennathur S, Heinecke JW. p-hydroxyphenylacetaldehyde, an aldehyde generated by myeloperoxidase, modifies phospholipid amino groups of low-density lipoprotein in human atherosclerotic intima. J Biol Chem 2000; 275:9957–9962.

[31] Lynch SM, Frei B. Reduction of copper, but not iron, by human low-density lipoprotein (LDL). Implications for metal ion-dependent oxidative modification of LDL. J Biol Chem 1995;270:5158–5163.

[32] Aviram M, Rosenblat M, Etzioni A, Levy R. Activation of NADPH oxidase required for macrophage-mediated oxidation of low-density lipoprotein. Metabolism 1996; 45:1069–1079.

[33] Abuja PM, Albertini R, Esterbauer H. Simulation of the induction of oxidation of low-density lipoprotein by high copper concentrations: Evidence for a nonconstant rate of initiation. Chem Res Toxicol 1997;10:644–651.

[34] Burkitt MJ. A critical overview of the chemistry of copper-dependent low-density lipoprotein oxidation: Roles of lipid hydroperoxides, alpha-tocopherol, thiols, and ceruloplasmin. Arch Biochem Biophys 2001;394:117–135.

[35] Fuhrman B, Shiner M, Volkova N, Aviram M. Cell-induced copper ion-mediated low-density lipoprotein oxidation increases during *in vivo* monocyte-to-macrophage differentiation. Free Radic Biol Med 2004;37:259–271.

[36] Cadenas E, Sies H. The lag phase. Free Radic Res 1998;28:601–609.

[37] Eiserich JP, Hristova M, Cross CE, Jones AD, Freeman BA, Halliwell B, van der Vliet A. Formation of nitric oxide-derived inflammatory oxidants by myeloperoxidase in neutrophils. Nature 1998;391:393–397.

[38] Beckmann JS, Ye YZ, Anderson PG, Chen J, Accavitti MA, Tarpey MM, White CR. Extensive nitration of protein tyrosines in human atherosclerosis detected by immunohistochemistry. Biol Chem Hoppe-Seyler 1994;375:81–88.

[39] Moore KP, Darley-Usmar V, Morrow J, Roberts LJ, 2nd. Formation of F2-isoprostanes during oxidation of human low-density lipoprotein and plasma by peroxynitrite. Circ Res 1995;77:335–341.

[40] Hayek T, Oiknine J, Brook JG, Aviram M. Increased plasma and lipoprotein lipid peroxidation in apo E-deficient mice. Biochem Biophys Res Commun 1994; 201:1567–1574.

[41] Maor I, Kaplan M, Hayek T, Vaya J, Hoffman A, Aviram M. Oxidized monocyte-derived macrophages in aortic atherosclerotic lesion from apolipoprotein E-deficient mice and from human carotid artery contain lipid peroxides and oxysterols. Biochem Biophys Res Commun 2000;269:775–780.

[42] Vaya J, Aviram M, Mahmood S, Hayek T, Grenadir E, Hoffman A, Milo S. Selective distribution of oxysterols in atherosclerotic lesions and human plasma lipoproteins. Free Radic Res 2000;34:485–497.

[43] Rosenblat M, Aviram M. Oxysterol-induced activation of macrophage NADPH-oxidase enhances cell-mediated oxidation of LDL in the atherosclerotic apolipoprotein E deficient mouse: Inhibitory role for vitamin E. Atherosclerosis 2002;160:69–80.

[44] Buege JA, Aust SD. Microsomal lipid peroxidation. Methods Enzymol 1978;52:302–310.